Original Paper

Annals of Neurosciences

Ann Neurosci 2018;25:210–218
DOI: 10.1159/000488022

Received: May 19, 2017
Accepted after revision: February 23, 2018
Published online: July 24, 2018

Comparative Morphometry of the Wisconsin Miniature Swine™ Thoracic Spine for Modeling Human Spine in Translational Spinal Cord Injury Research

Gurwattan Singh Miranpuri[a] Dominic T. Schomberg[a, b] Patricia Stan[a] Abhishek Chopra[a] Seah Buttar[a] Aleksandar Wood[b] Alexandra Radzin[a] Jennifer J. Meudt[b] Daniel K. Resnick[a] Dhanansayan Shanmuganayagam[b]

[a]Department of Neurological Surgery, University of Wisconsin School of Medicine and Public Health, Madison, WI, USA; [b]Department of Animal Sciences, Biomedical and Genomic Research Group, University of Wisconsin-Madison, Madison, WI, USA

Keywords
Animal models · Spinal cord injury · Miniature swine · Thoracic vertebrae · Spine anatomy · Swine models

Abstract
Background/Aims: Spine and spinal cord pathologies and associated neuropathic pain are among the most complex medical disorders to treat. While rodent models are widely used in spine and spinal cord research and have provided valuable insight into pathophysiological mechanisms, these models offer limited translatability. Thus, studies in rodent models have not led to the development of clinically effective therapies. More recently, swine has become a favored model for spine research because of the high congruency of the species to humans with respect to spine and spinal cord anatomy, vasculature, and immune responses. However, conventional breeds of swine commonly used in these studies present practical and translational hurdles due to their rapid growth toward weights well above those of humans. ***Methods:*** In the current study, we evaluated the suitability of a human-sized breed of swine developed at the University of Wisconsin-Madison, the Wisconsin Miniature Swine™ (WMS™), in the context of thoracic spine morphometry for use in research to overcome limitations of conventional swine breeds. The morphometry of thoracic vertebrae (T1–T15) of 5–6 months-old WMS was analyzed and compared to published values of human and conventional swine spines. ***Results:*** The key finding of this study is that WMS spine more closely models the human spine for many of the measured vertebrae parameters, while being similar to conventional swine in respect to the other parameters. ***Conclusion:*** WMS provides an improvement over conventional swine for use in translational spinal cord injury studies, particularly long-term ones, because of its slower rate of growth and its maximum growth being limited to human weight and size.

KARGER

E-Mail karger@karger.com
www.karger.com/aon

Dr. Dhanansayan Shanmuganayagam, PhD
Department of Animal Sciences
Biomedical and Genomic Research Group, University of Wisconsin-Madison
1675 Observatory Drive, Rm 666, Madison, WI 53706 (USA)
E-Mail dshanmug@wisc.edu

Introduction

Spinal cord injury (SCI) has a worldwide incidence of 1 in 25,000 and a total prevalence of around 276,000 patients in the United States alone [1]. In addition to functional disability, up to 70% of these patients are disproportionately affected by neuropathic pain (NP). Annual expenditures for treatment, care, and rehabilitation of SCI patients reach up to USD 10 billion [2]. Consistently effective therapies for SCI and for the management of NP have not been attained. While many promising molecular, gene, and cell therapies are being explored for SCI, advancement of these therapies to the clinical setting is hampered by a gap that exists between early research and clinical testing. Most SCI research occurs in small animal models such as mice [3–6] and rats [7–10]. However, no therapy shown to be safe and effective in rodent studies has advanced through clinical trials for treating human SCI [11]. A large animal model, such as the swine, may overcome many of the translational weaknesses of small animal models [12].

The genetic, anatomical, physiological, and pathophysiological proximity of the swine to human, and the similar spinal cord anisotropy, surface to volume ratios, and nerve tract organization, make swine an ideal model for preclinical studies of SCI. We have published a review concluding that swine, next to non-human primates, best models humans with respect to (1) spine and spinal cord anatomy, (2) spinal vasculature, (3) immune responses, and (4) assessment of higher neural function, and are suited for advancing the development of novel delivery systems and therapies in a translational manner [12]. Previous studies of the spine in swine found it to be an appropriate biomechanical model for the human spine [13, 14]. Other biomechanical studies comparing spinal segments from swine, sheep, goat, bovine, and deer further support the use of swine spine models but lacked precise geometrical data [15–17]. However, more recent studies have now included anatomical dimensions of the swine cervical, thoracic, and lumbar vertebrae [13, 18–20].

Most swine models of SCI utilize conventional breeds of swine [12]. These conventional breeds typically reach 100 kg (220 lb.) by 4–5 months of age and 249–306 kg (550–675 lb.) at full maturity and thus pose challenges in the biomedical research setting [21, 22]. In contrast, miniature swine breeds such as the Wisconsin Miniature Swine™ (WMS™) developed at the University of Wisconsin-Madison, range from 25 to 50 kg (55–110 lb.) at 4 months of age and 68–91 kg (150–200 lb.) at full maturity, approximating the weight of an average human. WMS can also maintain these adult human weights, while conventional breeds grow at a rate that renders them impractical for use in studies longer than a month duration and for studies using clinical imaging modalities such as MRI, CT, and PET. The disparity in growth rate also applies to the growth and development of the spine and spinal cord. In the context of SCI, the rapidly growing spine and spinal cord of conventional swine do not anatomically and physiologically model the comparatively static nature of the injured spine and spinal cord of a human adult. Additionally, miniature swine more accurately model human vascular anatomy, physiology, and pathophysiology [22], an aspect of biology that is important to the study of SCI. Given these advantages, the WMS is being increasingly considered for SCI studies. However, the comparative morphometry of the WMS spine has not yet been established. In this manuscript, we perform a morphometric analysis of the thoracic region of WMS spine and compare it to previously published reference values of human and conventional swine spines.

Methods

Swine Spine Source

All experiments involving animals were conducted under protocols approved by the University of Wisconsin-Madison Institutional Animal Care and Use Committee in accordance with published NIH and USDA guidelines. Five to sixmonth-old WMS (approximately 50 kg) bred and maintained at the Swine Research and Teaching Center (SRTC; University of Wisconsin-Madison) were euthanized (by electrical stunning of the brain followed by exsanguination) and their vertebral columns were dissected out from the body and kept frozen at –20 °C until use in morphometric studies.

Anatomical Dimensions

Extraneous soft tissue was removed from each thoracic vertebra using scalpel and forceps. Measurements were taken with calipers by 2 individuals, and averaged, using landmark references as previously published [13] (Fig. 1, Table 1). Analysis was confined to the T1–T15 thoracic region. While measurements of T2–T15 were performed on spines from all 5 swine, those of T1 were only collected from 3 of the spines.

Statistical Analysis

The measured parameters from the WMS spine were compared to those of human (55–84 years of age, mean = 72 years; mean height of 82 cm) and conventional swine (Landrace pigs; 4-month old; mean weight = 40 kg) that were previously published [13]. Welch's *t* test was performed using the equations below to identify statistically significant differences between WMS and human spines, and between WMS and conventional swine spines. We assumed normal distribution when using previously published data [13] and unequal variances between the compared data sets.]

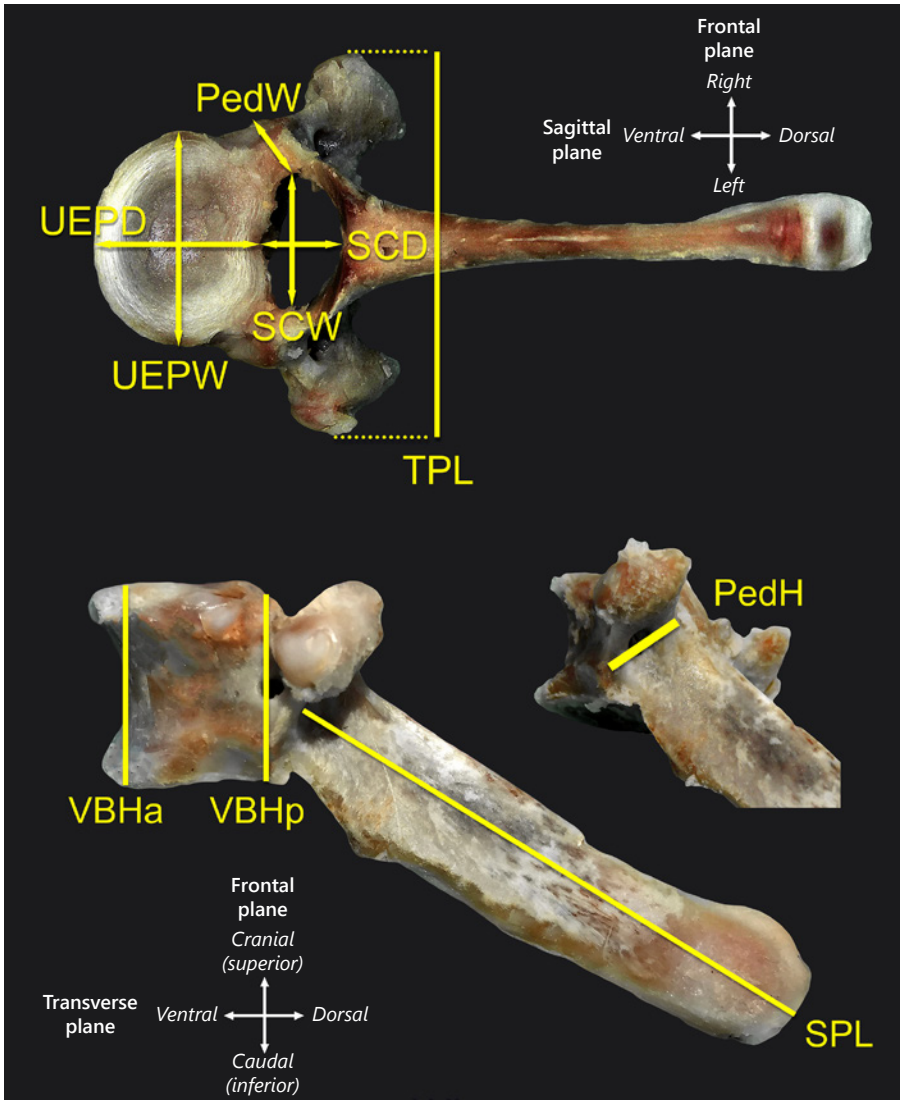

Fig. 1. Anatomical dimensions measured from each vertebra of WMS. Abbreviations are explained in Table 1. Representative T6 vertebrae shown.

$$t = \frac{\underline{X}_1 - \underline{X}_2}{s_{\underline{\Delta}}}$$

$$s_{\underline{\Delta}} = \sqrt{\frac{s_1^2}{n_1} + \frac{s_2^2}{n_2}}$$

$$d.f. \approx \frac{(\frac{s_1^2}{n_1} + \frac{s_2^2}{n_2})^2}{\frac{(\frac{s_1^2}{n_1})^2}{(n_1 - 1)} + \frac{(\frac{s_2^2}{n_2})^2}{(n_2 - 1)}}$$

where $\underline{X}$, s^2, n, and d.f. denote the sample mean, sample variance, sample size, and degrees of freedom respectively. The estimated *d.f.* values were rounded down for calculation of *p* values using

Table 1. Abbreviations of the vertebrae (T1–T12) parameters measured

Vertebrae parameter	Abbreviation
Vertebral body height, anterior	VBHa
Vertebral body height, posterior	VBHp
Upper end-plate width	UEPW
Upper end-plate depth	UEPD
Lower end-plate width	LEPW
Lower end-plate depth	LEPD
Spinal canal width	SCW
Spinal canal depth	SCD
Transverse process length	TPL
Spinous process length	SPL
Pedicle height (average of right and left)	PedH
Pedicle width (average of right and left)	PedW

2-tailed TDIST function of Microsoft Excel (software version 15.32). Significant differences were accepted at p value < 0.05. Data are presented as mean ± standard error of mean (SEM).

Results

Vertebral Body Height Dimensions

Anterior and posterior vertebral body height (VBHa and VBHp respectively) generally increases from T6–T15 in all species (Fig. 2). WMS VBHa values are significantly different from human from T1–T3 and T12, while VBHp values are significantly different at T2, T3, T10, and T12. WMS VBHa values are significantly different from conventional swine at T12–T15 and VBHp values are significantly different in most vertebrae. WMS VBHa means are closer to human than conventional swine from T9–T12 and in VBHp from T4–T12.

End-Plate Dimensions

Upper and lower end-plate widths (UEPW and LEPW) and depths (UEPD and LEPD) generally increased from T1–T15, with the rate of change being more pronounced in humans (Fig. 2). The WMS values for these parameters are significantly different from human except for T1 UEPD. While the patterns of difference are similar to those between human and conventional swine, most measurements (UEPW, LEPW, and LEPD) in WMS are more similar to those of human when compared to similarities between conventional swine and human.

Spinal Canal Dimensions

The spinal canal of a human is significantly wider and deeper than both the WMS and conventional swine spinal canal (Fig. 3). The human spinal canal width (SCW) values show narrowing width from T1–T4 and widening from T10–T12. Both swine SCW and spinal canal depth (SCD) values show narrowing T1–T3 and then remain relatively constant. WMS values for SCW are significantly different from those of conventional swine and SCD values are significantly different at T10–T12. WMS mean values are all closer to human than those of conventional swine.

Pedicle Width and Height

WMS pedicle width is significantly different from humans at T6 and T12 and significantly different from conventional swine at T12–T15 (Fig. 3). WMS pedicle height (PedH) is significantly different from that of both human and conventional swine species; WMS mean values are larger and conventional swine values are smaller than those of human.

Process Length

Spinous process lengths (SPL) generally decrease over the thoracic vertebrae in both swine models, while that of human first increase from T1–T6 before decreasing (Fig. 3). WMS SPL is significantly different from that of human from T1–T7 and significantly different from conventional swine at every vertebra. Transverse process length in both WMS and conventional swine is significantly different and with smaller mean values than that of humans. Transverse process length decreases proportionally down the thoracic spine in both species.

Discussion

The current study focused on the thoracic region of the spine, as many of the existing swine models of traumatic SCI commonly target this region for research. The key finding of this study is that the WMS™ spine more closely models the human thoracic spine than the spine of conventional swine does with respect to many of the measured vertebrae parameters. For all others, except VBHa (T1–T8), PedH (T1–T12), and SPL (T1–T12), WMS spine models the human spine similarly to conventional swine.

An effective animal model must accurately represent the complexities of the human spine, spinal cord, and the pathophysiology of injury to allow for the development and testing of therapies and delivery systems in a transalational manner [12]. To date, drug-based therapies for SCI and NP management have had limited efficacy in humans [23]. The heavy reliance on mouse [3–6, 24] and rat [7–10] models for SCI research has led to inaccurate assessment of the effectiveness of therapies and delivery methods, especially of those administered into the spinal cord. The large surface area to volume ratio and the small axial plane of the spinal cord in small animals result in the distribution of therapies that is significantly different from that in humans. In such models, simple diffusion drives pharmaceutical delivery, bathing a large segment of the spinal cord in the administered therapy. Therefore, promising therapies developed in rodents when advanced to humans often fail to demonstrate a substantial effect in the human spinal cord, for example, where simple diffusion does not deliver the therapy into portions of the transverse spinal cord [23]. Thus, larger animal models such as the swine that more closely mimic human spine and spinal cord anatomy and size enable more accurate assessment of the efficacy of therapies delivered into the spinal cord (Fig. 4). They also provide the platform on which advanced delivery methods, such as convection enhanced delivery, which

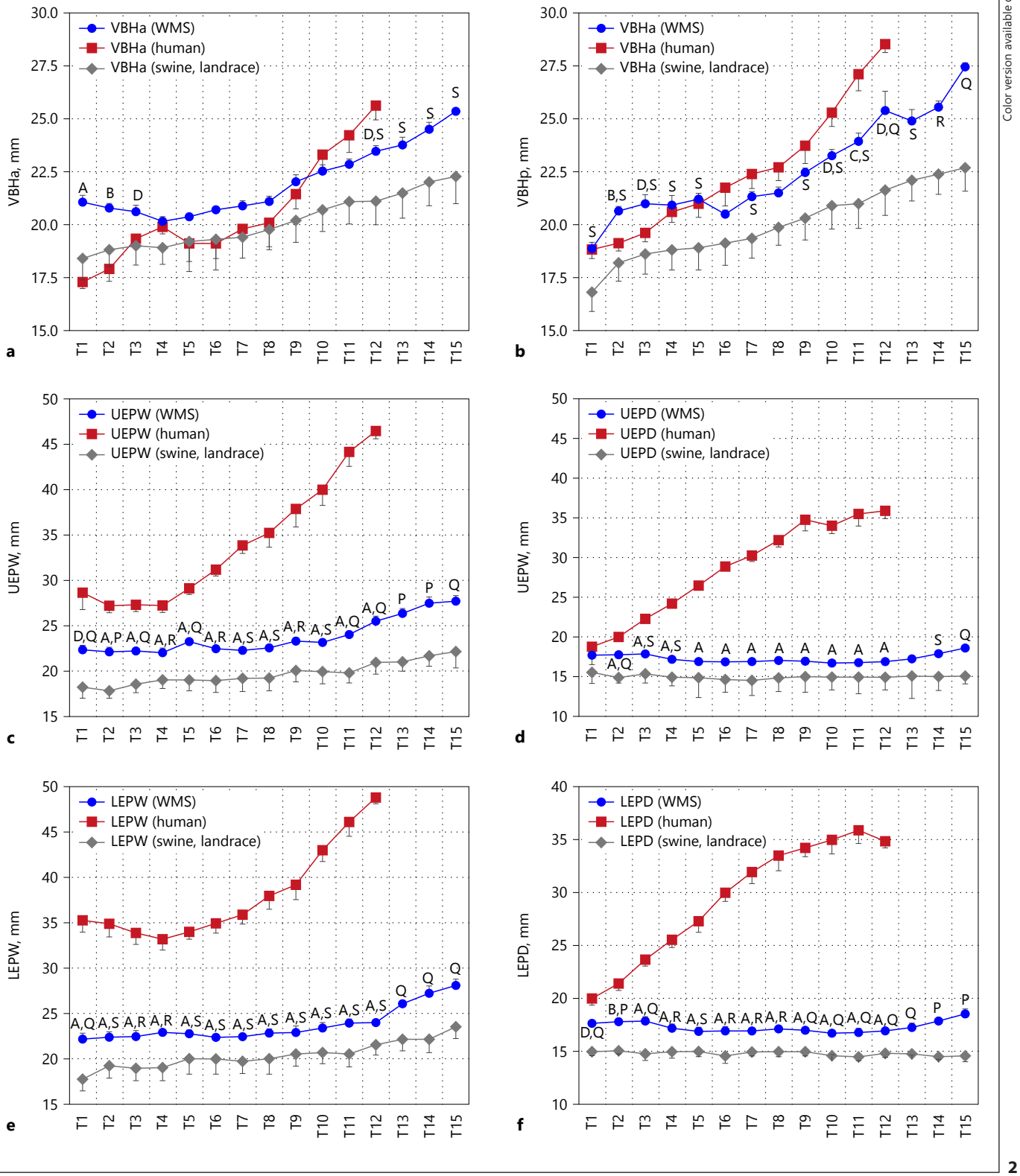

Color version available online

2

(For legend see next pages.)

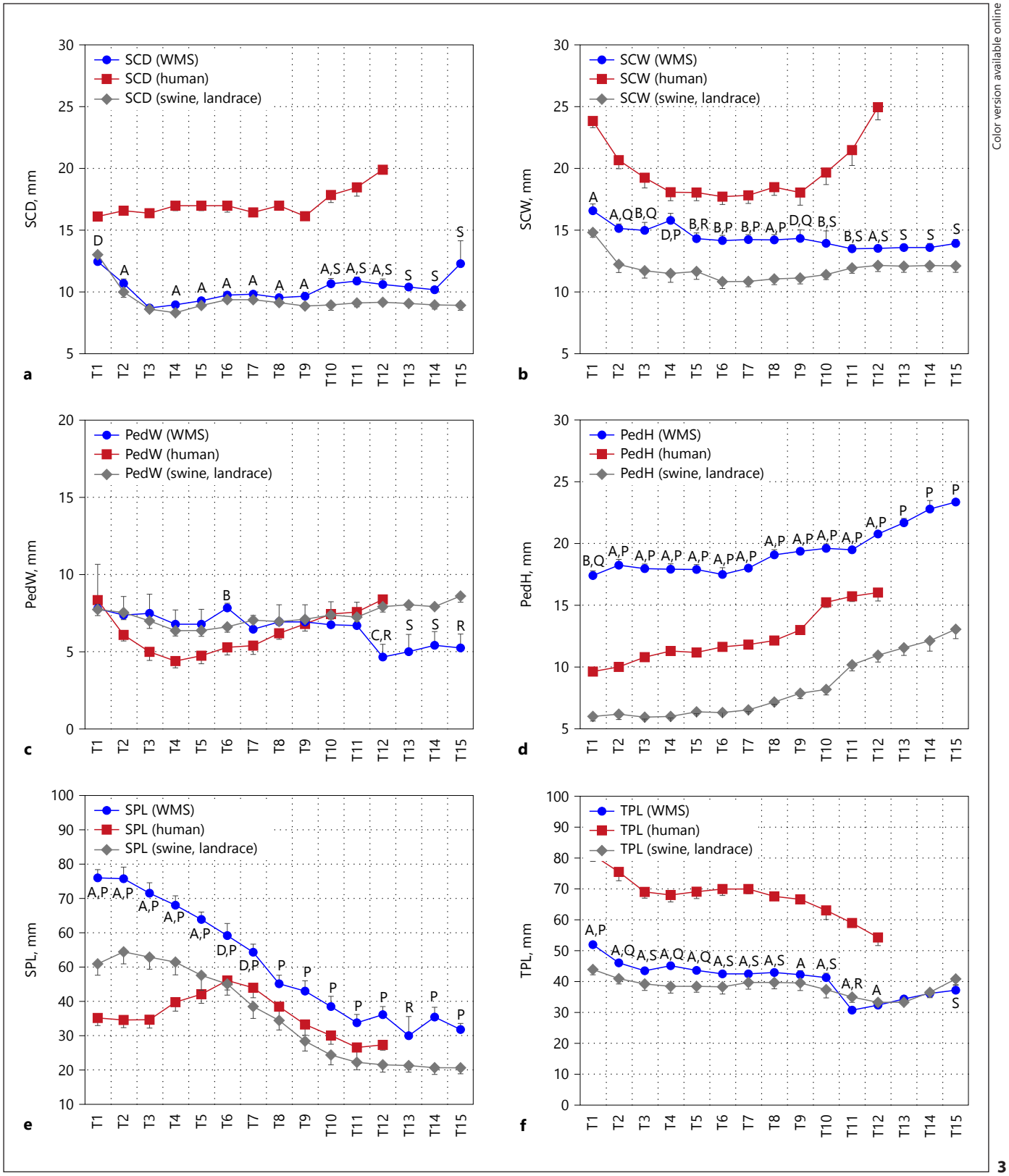

Color version available online

3

(For legend see next pages.)

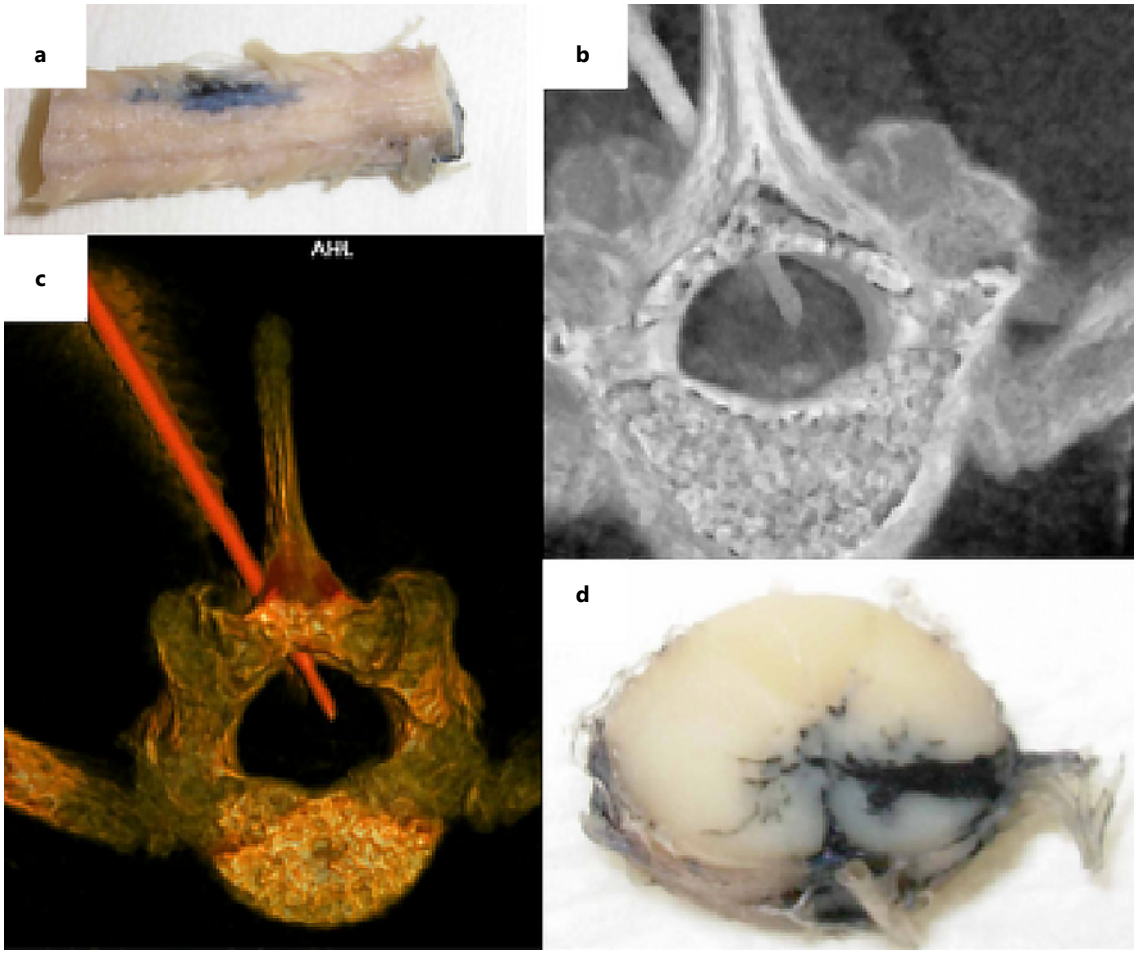

Fig. 4. Studies of percutaneous delivery of India ink (to simulate drug delivery) into the spinal cord of a conventional swine. The figure shows representative images from past studies performed to explore spinal cord drug delivery approaches. **a** External anatomy of the infused spinal cord. **b** Computed tomography (CT) of the spine and spinal cord during delivery via percutaneous catheter. **c** Images of the vertebral bone and delivery catheter demonstrating the approach for subsequent. **d** Delivery into a targeted region within the ventral spinal cord.

Fig. 2. Figure shows (**a**) vertebral body height anterior (VBHa), (**b**) vertebral body height posterior (VBHp), (**c**) upper end-plate width (UEPW), (**d**) upper end-plate depth (UEPD), (**e**) lower end-plate width (LEPW), (**f**) lower end-plate depth (LEPD), measurements in T1–T12 segments from spine of the Wisconsin Miniature Swine (WMS), and compared to published values [13] of spine of humans and a conventional swine breed (Landrace). Letters A–D denote statistically significant differences ($p < 0.001$, $p < 0.005$, $p < 0.01$, and $p < 0.05$, respectively) in measurements between WMS and human spines at the corresponding vertebral segment (T1–T10). Letters P–S denote statistically significant differences ($p < 0.001$, $p < 0.005$, $p < 0.01$, and $p < 0.05$ respectively) in measurements between WMS and conventional swine at the corresponding vertebral segment (T1–T12). The data are presented as mean ± SEM.

Fig. 3. Figure shows (**a**) spinal canal dimensions (SCD), (**b**) spinal canal width (SCW), (**c**) pedicle width (PedW), (**d**) pedicle height (PedH), (**e**) spinous process length (SPL), (**f**) transverse process length (TPL), measurements in T1–T12 segments from spine of the Wisconsin Miniature Swine (WMS), and compared to published values [13] of spine of humans and a conventional swine breed (Landrace). Letters A–D denote statistically significant differences ($p < 0.001$, $p < 0.005$, $p < 0.01$, and $p < 0.05$, respectively) in measurements between WMS and human spines at the corresponding vertebral segment (T1–T10). Letters P–S denote statistically significant differences ($p < 0.001$, $p < 0.005$, $p < 0.01$, and $p < 0.05$ respectively) in measurements between WMS and conventional swine at the corresponding vertebral segment (T1–T12). The data are presented as mean ± SEM.

show promise for targeted delivery of therapies into the brain [25–28], can be developed and refined for improving the effectiveness of therapies administered into the spinal cord [25, 29].

Although the swine has been increasingly recognized as a more translational SCI model, its use has been hampered by practical limitations often posed by the rapid growth rate of conventional swine breeds, especially when used in longer-term efficacy studies. The corresponding rate of growth of vertebrae also hampers proper testing of static corrective devices or hardware, such as pedicle screws. Thus, miniature swine breeds such as WMS with the slower rate of growth and human weights at maturity offer practical advantages over conventional breeds for SCI research. The current study provides the first morphometric characterization of the WMS spine and validation that the breed would provide an improvement over conventional swine for spine studies.

Acknowledgments

We would like to thank Kush Patel, Lisa Liu, Therese Howe, and Wesley Webster for their technical contributions to the study. We would also like to thank the Director (Dr. Thomas Crenshaw) and staff (Mr. Jamie Reichert, Dr. Ana Cecilia Escobar López, Mr. Sam Trace and Ms. Keri Graff) of the SRTC, the Facility Manager (Ms. Catherine Jobsis) and staff (Mr. Kim Trumble) of the Translational Research Facility, Mr. Robert Weyker and Dr. Michael Maroney (Attending Veterinarian) at the University of Wisconsin-Madison for their overall programmatic support of the research incorporated into this review.

Disclosure Statement

The authors declare that there are no competing financial interests to disclose.

Funding Sources

The research described in the manuscript was supported by discretionary funds from research programs of Drs. Resnick and Shanmuganayagam, and an equipment grant provided to Dr. Gurwattan Singh Miranpuri by Engineering Resource Group, Inc. (Florida, USA).

Author Contribution

Authors contributed to the conception or design (G.S.M., D.T.S., D.K.R., and D.S.); data acquisition, analysis, or interpretation (G.S.M., D.T.S., P.S., A.C., S.B., A.W., A.R., J.J.M., D.K.R., and D.S.); drafting the manuscript (G.S.M., D.T.S., P.S., A.C., S.B., A.W., A.R., J.J.M., and D.S.); and critically revising the manuscript (G.S.M., D.T.S., A.W., and D.S.). All authors gave their final approval and agreed to be accountable for all aspects of work in ensuring that questions related to the accuracy or integrity of any part of the work are appropriately investigated and resolved.

References

1 National Spinal Cord Injury Statistical Center. Spinal Cord Injury Facts and Figures at a Glance, 2016. [cited January 2, 2017]; https://www.nscisc.uab.edu.

2 Ackery A, Tator C, Krassioukov A: A global perspective on spinal cord injury epidemiology. J Neurotrauma 2004;21:1355–1370.

3 Gaudet AD, Mandrekar-Colucci S, Hall JC, Sweet DR, Schmitt PJ, Xu X, Guan Z, Mo X, Guerau-de-Arellano M, Popovich PG: miR-155 deletion in mice overcomes neuron-intrinsic and neuron-extrinsic barriers to spinal cord repair. J Neurosci 2016;36:8516–8532.

4 White SV, Czisch CE, Han MH, Plant CD, Harvey AR, Plant GW: Intravenous transplantation of mesenchymal progenitors distribute solely to the lungs and improve outcomes in cervical spinal cord injury. Stem Cells 2016;34:1812–1825.

5 Coll-Miro M, Francos-Quijorna I, Santos-Nogueira E, Torres-Espin A, Bufler P, Dinarello CA, Lopez-Vales R: Beneficial effects of IL-37 after spinal cord injury in mice. Proc Natl Acad Sci U S A 2016;113:1411–1416.

6 Butenschon J, Zimmermann T, Schmarowski N, Nitsch R, Fackelmeier B, Friedemann K, Radyushkin K, Baumgart J, Lutz B, Leschik J. PSA-NCAM positive neural progenitors stably expressing BDNF promote functional recovery in a mouse model of spinal cord injury. Stem Cell Res Ther 2016;7:11.

7 Miranpuri GS, Schomberg DT, Alrfaei B, King KC, Rynearson B, Wesley VS, Khan N, Obiakor K, Wesley UV, Resnick DK: Role of matrix metalloproteinases 2 in spinal cord injury-induced neuropathic pain. Ann Neurosci 2016;23:25–32.

8 Liu G, Fan G, Guo G, Kang W, Wang D, Xu B, Zhao J: FK506 attenuates the inflammation in rat spinal cord injury by inhibiting the activation of NF-κB in microglia cells. Cell Mol Neurobiol 2017;37:843–855.

9 Kloefkorn HE, Pettengill TR, Turner SM, Streeter KA, Gonzalez-Rothi EJ, Fuller DD, Allen KD: Automated gait analysis through hues and areas (AGATHA): a method to characterize the spatiotemporal pattern of rat gait. Ann Biomed Eng 2017;45:711–725.

10 Wu C, Chen J, Liu Y, Zhang J, Ding W, Wang S, Bao G, Xu G, Sun Y, Wang L, Chen L, Gu H, Cui B, Cui Z: Upregulation of PSMB4 is associated with the necroptosis after spinal cord injury. Neurochem Res 2016;41:3103–3112.

11 Kwon BK, Streijger F, Hill CE, Anderson AJ, Bacon M, Beattie MS, Blesch A, Bradbury EJ, Brown A, Bresnahan JC, Case CC, Colburn RW, David S, Fawcett JW, Ferguson AR, Fischer I, Floyd CL, Gensel JC, Houle JD, Jakeman LB, Jeffery ND, Jones LA, Kleitman N, Kocsis J, Lu P, Magnuson DS, Marsala M, Moore SW, Mothe AJ, Oudega M, Plant GW, Rabchevsky AS, Schwab JM, Silver J, Steward O, Xu XM, Guest JD, Tetzlaff W: Large animal and primate models of spinal cord injury for the testing of novel therapies. Exp Neurol 2015;269:154–168.

12 Schomberg DT, Miranpuri GS, Chopra A, Patel K, Meudt JJ, Tellez A, Resnick DK, Shanmuganayagam D: Translational relevance of swine models of spinal cord injury. J Neurotrauma 2017;34:541–551.
13 Busscher I, Ploegmakers JJ, Verkerke GJ, Veldhuizen AG: Comparative anatomical dimensions of the complete human and porcine spine. Eur Spine J 2010;19:1104–1114.
14 Busscher I, van der Veen AJ, van Dieen JH, Kingma I, Verkerke GJ, Veldhuizen AG: In vitro biomechanical characteristics of the spine: A comparison between human and porcine spinal segments. Spine (Phila Pa 1976) 2010;35: E35–E42.
15 Bozkus H, Crawford NR, Chamberlain RH, Valenzuela TD, Espinoza A, Yuksel Z, Dickman CA: Comparative anatomy of the porcine and human thoracic spines with reference to thoracoscopic surgical techniques. Surg Endosc 2005;19:1652–1665.
16 Kettler A, Liakos L, Haegele B, Wilke HJ: Are the spines of calf, pig and sheep suitable models for pre-clinical implant tests? Eur Spine J 2007;16:2186–2192.
17 Kumar N, Kukreti S, Ishaque M, Mulholland R: Anatomy of deer spine and its comparison to the human spine. Anat Rec 2000;260:189–203.
18 Dath R, Ebinesan AD, Porter KM, Miles AW: Anatomical measurements of porcine lumbar vertebrae. Clin Biomech (Bristol, Avon) 2007;22:607–613.
19 Sheng SR, Wang XY, Xu HZ, Zhu GQ, Zhou YF: Anatomy of large animal spines and its comparison to the human spine: a systematic review. Eur Spine J 2010;19:46–56.
20 Sheng SR, Xu HZ, Wang YL, Zhu QA, Mao FM, Lin Y, Wang XY: Comparison of cervical spine anatomy in calves, pigs and humans. PLoS One 2016;11:e0148610.
21 Swindle MM, Smith AC, Laber-Laird K, Dungan L: Swine in biomedical research: management and models. ILAR Journal 1994;36:1–5.
22 Schomberg DT, Tellez A, Meudt JJ, Brady DA, Dillon KN, Arowolo FK, Wicks J, Rousselle SD, Shanmuganayagam D: Miniature swine for preclinical modeling of complexities of human disease for translational scientific discovery and accelerated development of therapies and medical devices. Toxicol Pathol 2016;44:299–314.
23 Vranken JH: Mechanisms and treatment of neuropathic pain. Cent Nerv Syst Agents Med Chem 2009;9:71–78.
24 Tateda S, Kanno H, Ozawa H, Sekiguchi A, Yahata K, Yamaya S, Itoi E: Rapamycin suppresses microglial activation and reduces the development of neuropathic pain after spinal cord injury. J Orthop Res 2017;35:93–103.
25 Miranpuri G, Hinchman A, Wang A, Schomberg D, Kubota K, Brady M, Raghavan R, Bruner K, Brodsky E, Block W, Grabow B, Raschke J, Alexander A, Ross C, Simmons H, Sillay K: Convection enhanced delivery: a comparison of infusion characteristics in ex vivo and in vivo non-human primate brain tissue. Ann Neurosci 2013;20:108–114.
26 Sillay K, Hinchman A, Kumbier L, Schomberg D, Ross C, Kubota K, Brady M, Brodsky E, Miranpuri G, Raghavan R: Strategies for the delivery of multiple collinear infusion clouds in convection-enhanced delivery in the treatment of parkinson's disease. Stereotact Funct Neurosurg 2013;91:153–161.
27 Sillay K, Schomberg D, Hinchman A, Kumbier L, Ross C, Kubota K, Brodsky E, Miranpuri G: Benchmarking the ERG valve tip and MRI interventions smart flow neurocatheter convection-enhanced delivery system's performance in a gel model of the brain: Employing infusion protocols proposed for gene therapy for parkinson's disease. J Neural Eng 2012;9:026009.
28 Schomberg D, Wang A, Marshall H, Miranpuri G, Sillay K: Ramped-rate vs continuous-rate infusions: an in vitro comparison of convection enhanced delivery protocols. Ann Neurosci 2013;20:59–64.
29 Lonser RR, Gogate N, Morrison PF, Wood JD, Oldfield EH: Direct convective delivery of macromolecules to the spinal cord. J Neurosurg 1998;89:616–622.